An examination of land use impacts of sea level rise induced flooding

Jie Song[1], Xinyu Fu[1], Yue Gu[1], Yujun Deng[1], Zhong-Ren Peng[1]

[1]Department of Urban and Regional Planning, College of Design, Construction, and Planning, University of Florida, POB 115706, 32611, USA

Correspondence to: Zhong-Ren Peng (zpeng@ufl.edu)

Abstract. Coastal regions are under intense developments because of their biodiversity and economic attractiveness. Meanwhile, these places are highly vulnerable to coastal hazards that are associated with sea level rise. Continuing urban development in these coastal areas that are prone to flooding increasingly poses unnecessary risk to their residents. While overwhelming efforts have been made to investigate coastal land use changes, few studies have simultaneously explored the urban growth dynamics and its interaction with coastal hazards. This paper applied the cellular automaton-based SLEUTH model to calibrate historical urban growth patterns from 1974 to 2013 in Bay County, Florida, USA. Three scenarios of urban growth---historical trend, compact development, and urban sprawl---up to 2080 were predicted by applying the calibrated SLEUTH model. To assess the effects of different policies, we developed four excluded layers: no regulations, flooding-risk mitigation based on the whole study region, conservational/agricultural land protection, and flooding-risk mitigation under the scenario of Areas More Likely to Experience Growth. We then evaluated how different urban growth patterns were oriented under these policies. Eventually, flooding maps were overlaid with future urban areas, and the exposure of different urban growth patterns to sea level rise induced flooding was examined. The findings suggest that if the coastal cities expand in a compact manner, areas vulnerable to flooding will increase compared with historical trend and urban sprawl scenarios. With respect to policies, if no regulations are implemented, on average the flooded area in 2080 would be more than 25 times under flooding-risk mitigation. The joint model can serve as a decision support tool to assist city officials, urban planners, and hazard mitigation teams in making informed decisions. The visualization results can be useful in public outreach regarding coastal communities' increasing risk to sea level rise induced flooding.

1 Introduction

Coastal areas are the most intensively exploited places where urban expansion largely alters natural landscape. As land-sea interfaces, however, coastal regions are featured by various conflicts between anthropogenic pressures and natural forces. Moreover, such conflicts have been exacerbated in recent years. While coastal zones increasingly attract population and investments, their communities become more aware of the intensified frequency of natural incidents. Climate change is likely to contribute to intensified hurricanes and floods (Hsu, 2014), rising sea level (IPCC, 2013), and other coastal hazards. More specifically, coastal flooding, land submergence, and saltwater intrusion may be worsened by sea level rise (SLR) (Nicholls & Cazenave, 2010). According to the fifth assessment report published by the Intergovernmental Panel on Climate Change

(IPCC) in 2013, by 2100 approximate 70% coastlines will experience rising sea levels. Yet, different stakeholders---residents, tourists, and developers---still compete for limited coastal resources, and the competition has been even more intense. Coastal areas attract more residential projects and infrastructure investments; oil and natural gas are extensively extracted in offshore regions (Felsenstein & Lichter, 2014). Since coastal zones are both vulnerable low-lying places and the battleground of conflicting interests, coordinating land uses, hazard mitigation, and different interests has become everlastingly important. The coordination, therefore, calls for effective tools to assist in the formulation of coastal management plans. Moreover, a pivotal part of these plans is spatial planning, which can be guided by identifying Land Use/Land Cover Changes (LULCC).

Various techniques have been applied to detect LULCC patterns. The class of Cellular Automaton (CA) models receive more attention around the world due to their simplicity and effectiveness in capturing complex urban dynamics (Akın, Clarke, & Berberoglu, 2014). The operationalization of CA in modelling urban phenomena was first introduced by Clarke et al. (1997). In their model each cell had a state which updated at every time step according to a predefined set of transitional rules. These rules took into account the current state of a cell and its neighbours as well as environmental constraints. A wide range of models and software packages have been developed since the introduction of CA. Santé et al. (2010) evaluated thirty-three CA related models and concluded that two widely applied models were SLEUTH and another package developed by White and Engelen (2000). SLEUTH has been adopted by urban researchers all over the world since 2000 (Project Gigalopolis, 2016). Its popularity among modellers is partly due to the following aspects: it is free and supported by a technical forum; it only requires six data inputs (i.e., slope, land use, exclusion, urban extent, transportation, and hillshade); it follows a well-documented calibration process (Sekovski et al., 2015); and it is computationally efficient. Recently, SLEUTH was improved by the incorporation of external information during the calibration. Rienow and Goetzke (2015) used support vector machine to enhance the predictive power of SLEUTH by developing probability-based excluded layers for future scenarios. Sakieh et al. (2015) applied multi-criterion evaluation method to develop suitability surfaces as excluded layers.

Based on historical urban expansion patterns, future land use could be simulated via scenario-based SLEUTH and other CA models. By applying a constrained CA model, Hansen (2010) simulated future land conditions under different emission scenarios developed by the IPCC (2013) and concluded that considerable areas in Aalborg would be exposed to potential flooding. Although the author incorporated adaptation strategies in his model, Hansen (2010) suggested that more radical strategies, such as population relocation and managed retreat, may be evaluated in future simulations. Likewise, Sekovski et al. (2015) assessed the impacts of coastal flooding upon urban growth using the SLEUTH model. Inouye et al. (2015) applied a comparative modelling approach to validate the importance of zoning in urban growth simulations. By applying the Dynamic EGO software, they stated that the development in ecological-economic zones may heighten future urban exposure to land sliding, intensified precipitation, SLR, and other coastal hazards. Their results provide actionable information to decision makers to develop relocation, planned retreat, and other adaptation policies. In addition, some researchers highlighted the importance of zoning information in SLEUTH applications. Akin et al. (2014) used current zoning maps as excluded layers and evaluated hindcasting-based calibration. Onsted and Chowdhury (2014) employed a historical zoning map in their SLEUTH model and suggested that land use zoning strongly influenced urban growth in Florida. While the majority of

SLEUTH applications focused on assessing prospective urban sprawl, compact development, and other growth patterns, the investigation of future land use exposure to coastal flooding received less attention. To the best of our knowledge, only two studies (Garcia & Loáiciga, 2014; Sekovski et al., 2015) attempted to couple land use predictions with marine flooding maps using SLEUTH. The combination of SLEUTH simulations and flooding hazard maps, however, should be prioritized in coastal land use modelling to better inform spatial management (Jeffrey A. Onsted & Chowdhury, 2014). Therefore, this study aims to evaluate the extent to which different urban growth patterns may be exposed to SLR induced flooding. Specifically, two research questions of this study are:

1. How may different urban growth patterns increase regional vulnerability to SLR induced flooding?
2. Would land use zoning and flooding mitigation plans help to steer prospective developments away from flood-prone regions?

This paper is organized as follows. Section 2 describes the study area and data collection. Following this, section 3 illustrates the modelling framework and outlines major steps for calibration, prediction, and the floodplain generation. In section 4 we present the calibration coefficients and discuss forecasting outcomes that were overlaid with flooding maps. Finally, section 5 offers a brief conclusion and provides the outlook for future research.

2 Study area and data description

2.1 Study area

The study region is located in northwest Florida and has long shorelines which form four bays along the Gulf Coast (Figure 1). It covers Bay County and some areas of Washington and Walton County. Its topographical features and past land use development render this region extremely susceptible to storm surges and hurricanes. For instance, considerable residential and commercial buildings encroached upon seafront areas in Panama City due to the absence of land use regulations in the past; as a result, urban growth largely occurs in flood-risk zones (Bay County Online, 2016). Historically, the study area has been hit by seventeen hurricanes since 1877 (Hurricanecity, 2015). Among these incidences, Hurricane Eloise in 1975 led to $23.1 million damages in structures, seawalls, and patios (Shows, 1978).

The economic activities and population profile of the study area increase its vulnerability to coastal hazards as well. Bay County highly relies on tourism related industries; specifically, restaurant and real estate are major industry sectors in Panama City. In Bay County the total spending on tourism as of June 2015, which was $121 million, had doubled since 2008 (Bureau of Economic and Business Research, 2015). Bay County has 10,222 firms, of which approximate 90% are small businesses. Small firms are susceptible to storm surge, flooding, and other environmental disasters (Runyan, 2006; Song, Peng, Zhao, &

Hsu, 2016). The overall population of Bay County is 168,852, around 30% of which come from two major coastal cities: Panama City and Panama City Beach (U.S. Census Bureau, 2015).

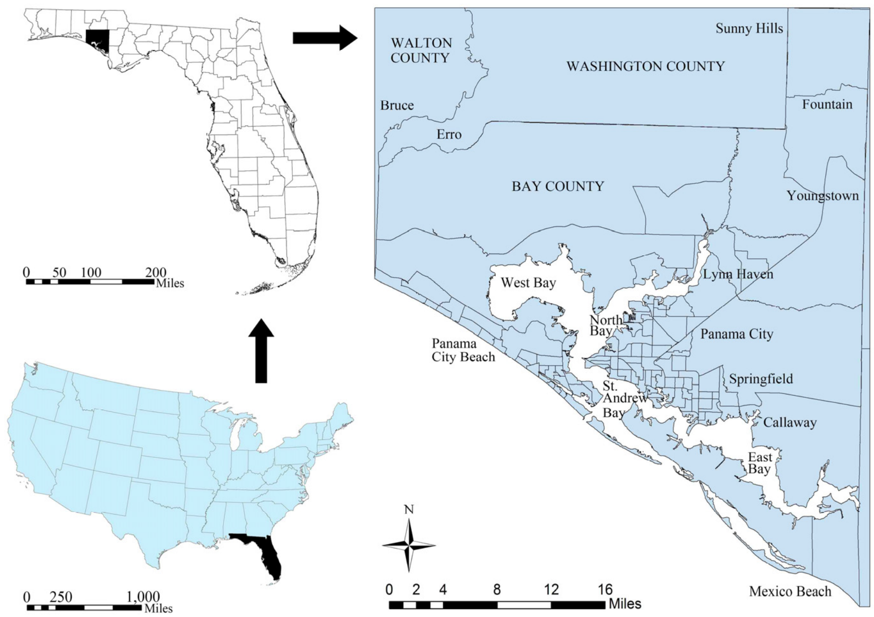

Figure 1. The study area.

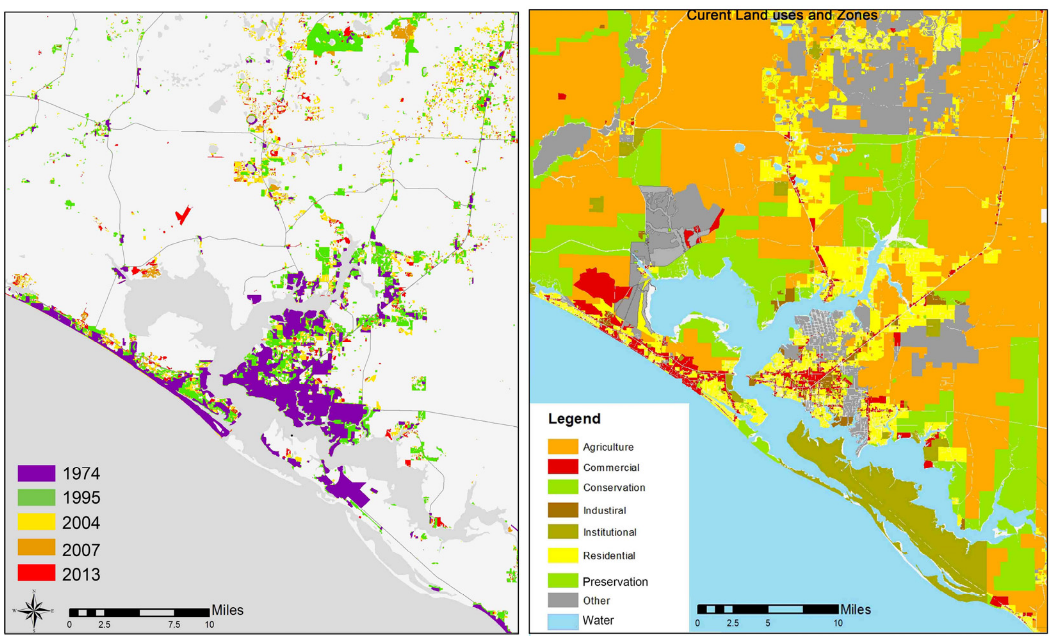

Figure 2. Historical urban changes (left) and current land uses and zones (right) for the study area.

2.2 Urban change and zoning

Figure 2 displays historical urban growth and current land use zoning for the study area. It indicates that urban extent expanded primarily in the southern part of Bay County. As shown in Figure 2, urban developments largely conform to historical trends. Substantial commercial and residential developments occur in two major cities: Panama City Beach and Panama City. In addition, a large piece of land in the north region is zoned for residential uses. This information suggests that local governments and planning agencies have taken measures to encourage inland developments. There exists, however, an apparent discrepancy between zoning and urban growth. Substantial built up areas have appeared in the Towns of Fountain and Youngstown. Nonetheless, such a pattern is not seen on the zoning map where only some areas are designated for the residential use in two towns. This inconsistency suggests that a comprehensive understanding of past land use changes is required to better inform prospective land use zoning.

2.3 Data description

Table 1. Sources and descriptions of data sets.

Data type	Year	Spatial resolution	Description and source
Urban extent	1974 1995 2004 2007 2013	Vector files	Land use/cover maps from Florida Geographic Data Library
Transportation network	2007 2013	Vector files	TIGER/Line® Shapefiles and TIGER/Line® Files
Slope	-	30 * 30 m	Converted from National Elevation Datasets of Geospatial Data Gateway from U.S. Natural Resources Conservation Service
Hillshade	-		
Exclusion	1996 2015	Vector files	Flood Insurance Rate Maps from Florida Geographic Data Library
	2016	Vector files	Land uses and zones from Bay County GIS online
Flooding maps	2030 2080	-	The estimates of sea level rise and sea surface temperature published by the IPCC

Land use and SLR data were prepared for this study. The land use data were comprised of five remotely sensed images on 1974, 1995, 2004, 2007, and 2013; these data were obtained from the Florida Geographic Data Library. These data sets were categorized into nine level-one land cover classes, among which the built-up land was coded as one, according to the Florida land use, cover and forms classification system published by the Florida Department of Transportation (1999). Flooding hazards and zoning information were also collected. Two Flood Insurance Rate Maps (FIRM), developed by the U.S. Federal Emergency Management Agency, were downloaded from the Florida Geographic Data Library. Current zoning map and the comprehensive plan for the study area were obtained from the online GIS websites of Bay County and Washington County. The zoning map specified exactly the degree to which different land uses were allowed for urban developments. According to the Bay County Comprehensive Plan (2009 to 2020), the zoning regulations are shown as follows:

-Developments were not allowed in the zone of conservation (for the preservation purpose), and impervious areas must be no more than 5%;

-In the zone of conservation (for the habitation purpose), impervious surface must be no more than 50%;

-In the zone of conservation (for the recreation purpose), impervious coverage must be no more than 10%; and

-In the zones of agriculture (for the timberland purpose) and agriculture, impervious areas must be no more than 10% and 25% respectively.

Finally, the data of projected SLR and sea surface temperatures were collected from the fourth assessment report published by the IPCC (2007). Table 1 displays detailed information regarding all data sets.

3 Method

3.1 An induction to SLEUTH

3.1.1 Background

SLEUTH is a packed C language-based source code that was developed by Dr. Keith C. Clarke at the Department of Geography, University of California Santa Barbara. The source code is freely available through its official website called "Project Gigalopolis" (http://www.ncgia.ucsb.edu/projects/gig/index.html).

SLEUTH is comprised of two modules: the Urban Growth Model and the Land Cover Deltatron Model. The Urban Growth Model mainly focuses on the urban/non-urban dynamics. It is more frequently adopted by SLEUTH users than the Land Cover Deltatron Model which investigates changes among different land cover classes. The Urban Growth Model is, therefore, a primary focus of this work. As mentioned, SLEUTH is a CA-based program which only relies on five inputs: urban, transportation, slope, hillshade, and exclusion, and thus it is moderately data driven. The family of CA models has gained more popularity than other modelling techniques. CA models are advantageous over other counterparts due to their spatial explicitness, flexible transitional rules, powerful performance with large data sets (Wagner, 1997), and easy integration with Geographical Information System (Santé et al., 2010). Furthermore, the SLEUTH model was selected for this research because of the following considerations. First, SLEUTH employs excluded layers as probability maps which specify developmental potentials over a study region (where the cell value of zero represents an attracting point for development, and 100 or higher reflects that development is strictly prohibited). Such a functionality makes SLEUTH an excellent platform for scenario-based studies (Leão, Bishop, & Evans, 2004; Jeffrey A. Onsted & Chowdhury, 2014). Second, SLEUTH uses five parameters---dispersion, breed, spread, road gravity, and slope---to establish transition rules which determine whether or not a cell is urbanized. Finally, the calibration process applies a "brute force" approach and is scientifically sound for regional studies (Jeffrey A Onsted & Clarke, 2011).

3.1.2 SLEUTH workflow

SLEUTH is a scale-independent CA model that updates the binary state of each cell per growth cycle. A growth cycle is one year and consists of four steps: spontaneous growth, new spreading centres, edge (organic) growth, road-influenced growth (Clarke et al., 1997). These transitional rules are controlled by one or more parameters that were mentioned previously. Each parameter, which has a value range of 1 – 100, is dimensionless and can be compared in terms of their contributions to overall growth. Specifically, the dispersion factor determines the probability by which a cell will be randomly selected for urbanization. The breed factor determines the likelihood by which a newly formed urban cluster will start its own growth cycles. The spread factor controls how likely outward growth will develop near an existing settlement. The road gravity factor demonstrates the influence of road systems upon urban growth by attracting new settlements that are within a certain distance of a road. Finally, the slope factor determines how likely a cell with steeper slope will be urbanized. Table 2 summarizes the relationships between transitional rules and five parameters.

Table 2. The relationships among a growth cycle, transitional steps, and controlling factors (Clarke et al., 1997).

Growth cycle	Transitional steps	Controlling factors	Description
1-1	Spontaneous growth	Dispersion	Random urbanization of cells
1-2	New spreading centers	Breed	Outward growth of new settlements formed in the spontaneous growth stage
1-3	Edge growth	Spread and slope	Outward growth of current settlements
1-4	Road-influenced growth	Road gravity, dispersion, breed, and slope	Growth of new settlements within a distance of existing transportation networks

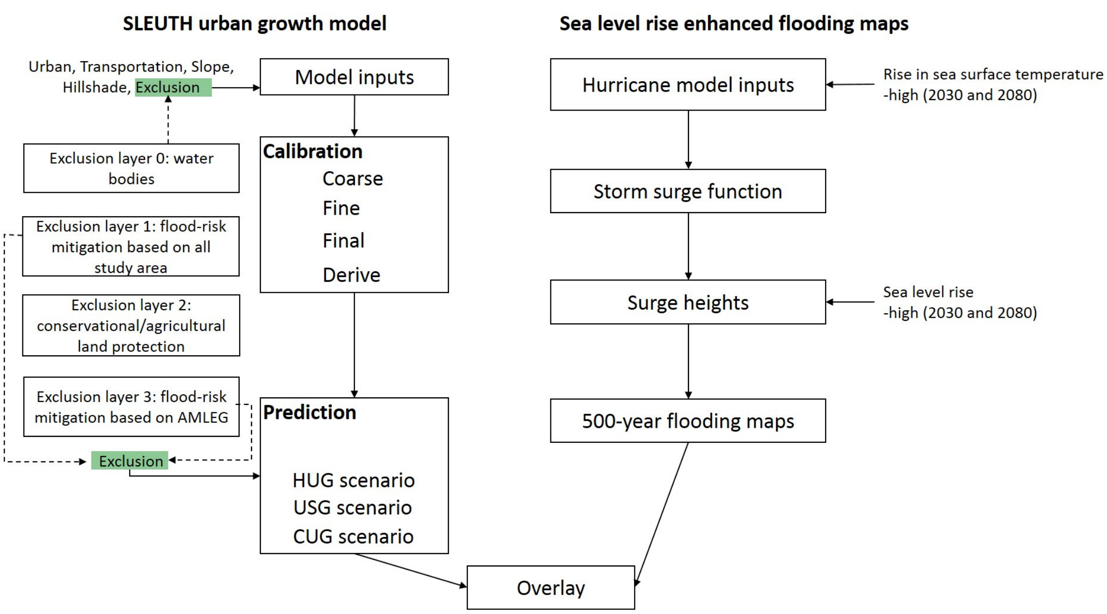

Figure 3. Overall study framework. HUG is historical urban growth; USG is urban sprawl growth; and CUG is compact urban growth.

The main workflow of a SLEUTH application includes input compilations, calibration based on historical urban growth, and predictions. In the Urban Growth Model, at least four maps of different dates which show discernible urban changes are required. Two road networks of different periods and one percentage-slope map are additional date sets. Finally, a hillshade map is used to enhance visualization performance, and water bodies can be embodied in this map. The goal of calibration is to select a combination of parameters that best simulate historical urban changes. This process, however, is enormously time-consuming if all combinations (up to 10 billion) are evaluated. Therefore, a four-stage calibration---coarse, fine, final, and derive----is applied to reduce computational time yet retains acceptable accuracy. Eventually, predictions with 100 Monte Carlo runs are conducted using the best-fit parameters. Full descriptions regarding model inputs, calibration, and predictions can be found in Project Gigalopolis (http://www.ncgia.ucsb.edu/projects/gig/Imp/implement.htm).

The workflow for this research was organized into four phases: 1) the preparation of input layers, 2) the calibration in the SLEUTH environment, 3) the predictions of urban growth up to 2080 under the combined scenarios of different developmental patterns and excluded layers, and 4) the overlaying of urban growth estimates and 500-year flooding maps that were induced by SLR. Figure 3 displays the overall research framework. The workflow was divided into two major tasks: the SLEUTH urban growth model and SLR induced flooding maps.

3.2 Urban growth model

3.2.1 Land use/cover related layers

All input data were processed in ArcGIS 10.3. Five land use maps in the vector format were converted into raster files using the nearest neighbourhood method for spatial resampling. Figure 4 shows urban changes of the study area from 1974 to 2013. Due to the absence of reliable records of transportation networks, only two most recent road maps were used. Because local roads may have very limited influence upon urban growth, only main arteries were extracted from original line files according to the MAF/TIGER Feature Class Code. These polylines were then converted into raster files using the nearest neighbour resampling method. Slope and hillshade were finally generated from the National Elevation Dataset using spatial analyst tool in ArcGIS.

3.2.2 The creation of E1 excluded layer

An excluded layer reflects the urbanization probabilities of cells. Its cell values range from 0 (unaffected) to 100 (entirely excluded) (Akın et al., 2014). Many publications have investigated how to use excluded layers to enhance calibration accuracy (Rienow & Goetzke, 2015; Sakieh et al., 2015) and evaluate policy scenarios (A. S. Mahiny & Clarke, 2012). Onsted and Clarke (2012) and Akin et al. (2014) recommended that different excluded layers should be used in calibration and prediction. The excluded layer for calibration is suggested to be at minimal restrictions in order to obtain more precise results for urban growth, according to Akin et al. (2014). Hence, this excluded layer (E0) only covers water bodies where urban developments are unrealistic (Figure 4). For prediction phases, however, three excluded layers were applied to represent flooding-risk mitigation based the whole region (E1), conservational/agricultural land protection (E2), and flooding-risk mitigation based on the Areas More Likely to Experience Growth (AMLEG) (E3).

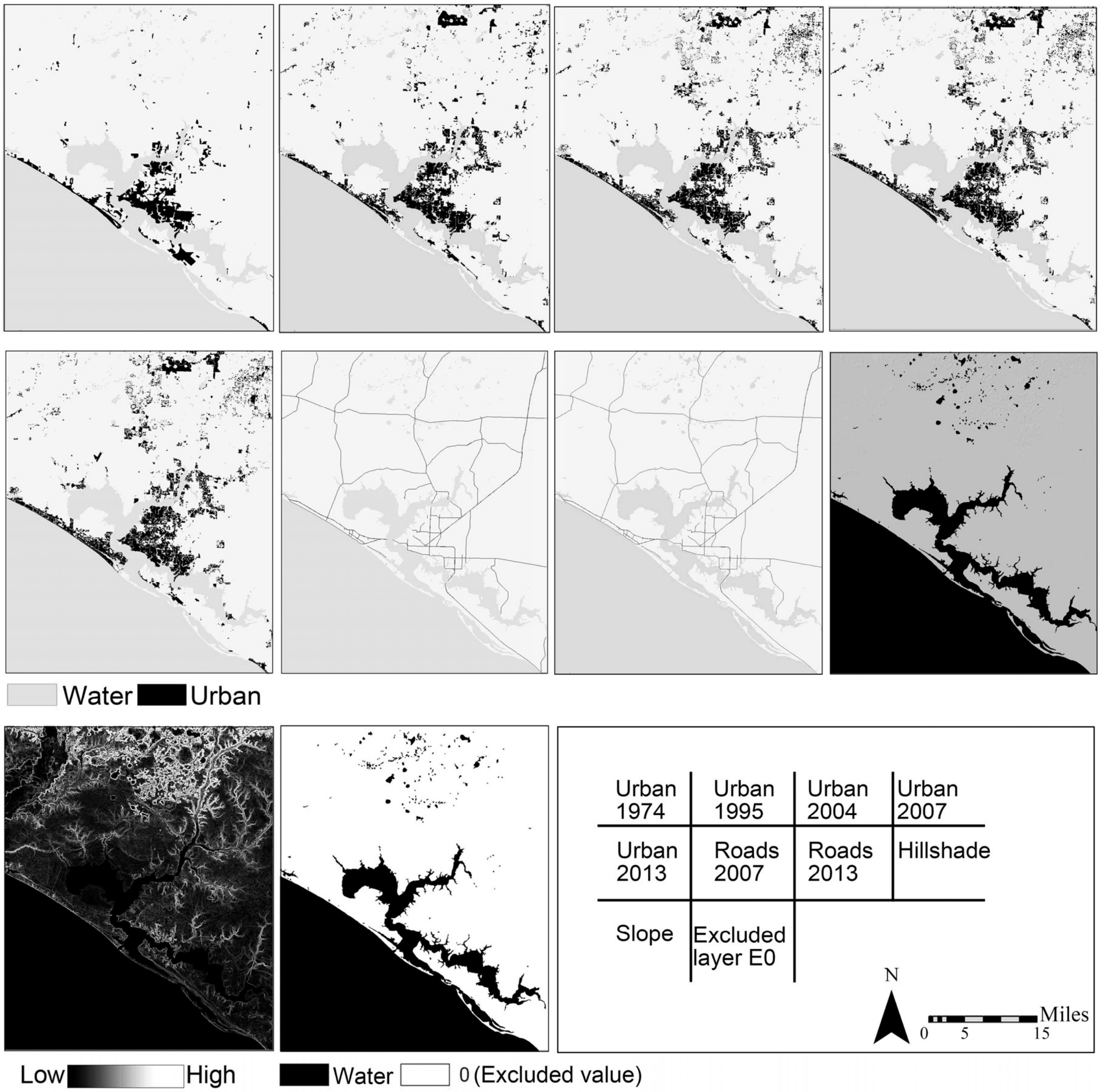

Figure 4. Urban layers, transportation, topographic and historic excluded layer (E1) for model inputs. For the excluded layer, higher value represents higher resistance to urban growth. The value range from 0 to 100.

E1 attempted to assess how likely urban growth appeared in the Special Flood Hazard Area (SFHA) which may be inundated by 100-year floods. Mandatory flood insurance must be purchased by land owners in these areas. Raising construction costs in high-risk regions may partly inhibit vulnerable urban growth. Therefore, E1 could represent a scenario which guides urban development towards less flood-prone areas. In order to avoid arbitrarily assigning values to excluded layers, Onsted et al. (2014) developed an approach to use historical zoning maps to calculate these values, which was adopted in the E1 excluded layer. Essentially, their method relies on the growth rates whereby urban development occurs in each zone. To retrieve past growth information, we selected 1996 Flood Insurance Rate Map (FIRM) as a reference layer and calculated the area of SFHA and non-SFHA zones as well as the amount of new urban areas from 1995 to 2013 in these zones.

Next, annual rate of urban growth in each zone was determined by Eq. (1):

$$g_n = 1 - ((1 - (\frac{G_n}{Z_n}))^{(1/T)}) \quad (1)$$

where G_n is the total actual urban growth in zone n (1 is SFHA and 2 is non-SFHA zone) from 1995 to 2013,

Z_n is total area of zone n according to the 1996 FIRM, and

T is the number of years, i.e., 18 years.

Finally, the growth rates were used to generate excluded value in the SFHA zone by Eq. (2):

$$E_{SFHA} = 100(1 - (\frac{g_1}{g_2})) \quad (2)$$

where g_1 and g_2 denote growth rates in SFHA and non-SFHA zone respectively. Table 3 indicates that the growth rate in low-risk areas was approximate three time in SFHA zone, suggesting that mandatory flooding insurance constrained urban expansion in vulnerable regions.

Table 3. The development of excluded value for E1 scenario (based on the whole study area).

Zones	New growth from 1995 to 2013 (hectares)	Total area (hectares)	Growth rate (‰)	Excluded value
Special Flood Hazard Area	665	92,054	0.4	68
Non-SFHA	4,901	216,095	1.3	0
Water bodies	-	-	-	100

Finally, E1 layer was created based on the 2015 FIRM and represented a managed growth plan that accounted for moderate protection from flooding risks (Figure 5).

3.2.3 The creation of E2 excluded layer

The 2020 Bay County Comprehensive Plan was published in 2009 and represented the most recent managed growth option for the study area. Hence, excluded values in the E2 layer were weighted according to this plan and modified based on the work of Akin et al. (2014). Specifically, a cell value of 100 was assigned to water bodies, 95 to the conservation/preservation zones, 50 to the conservation/recreation and agriculture/timberland areas, 25 to other agricultural areas and conservation/habitation zones, and 0 to all other areas (Figure 6).

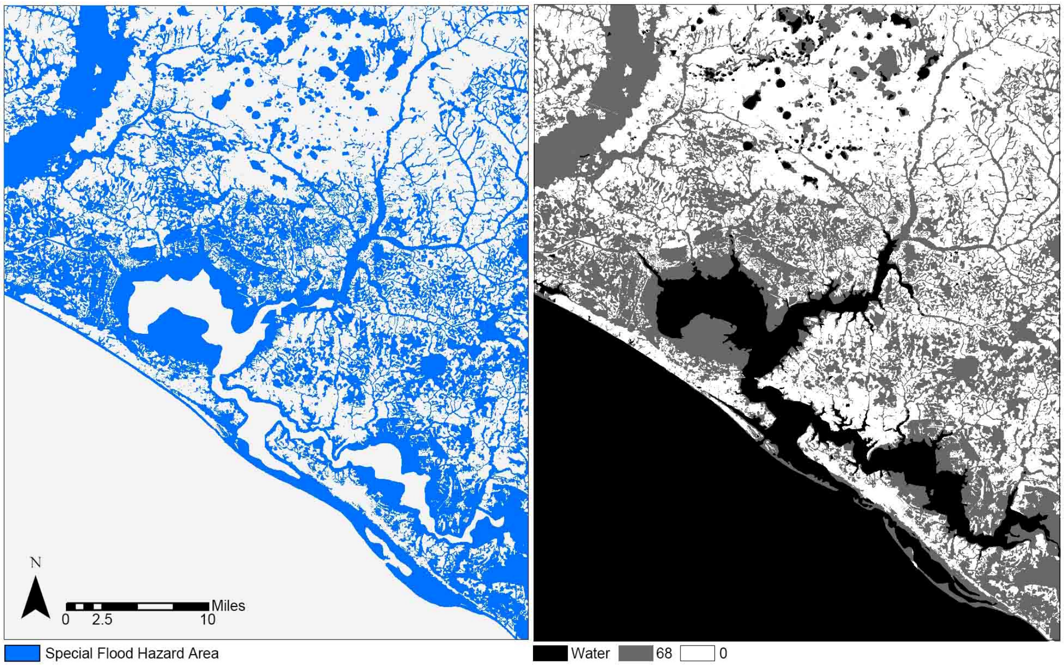

Figure 5. Special Flood Hazard Area in 2015 (left) and the E1 excluded layer (right) (based on the whole study area). For the excluded layer, higher value represents higher resistance to urban growth. The value ranges from 0 to 100.

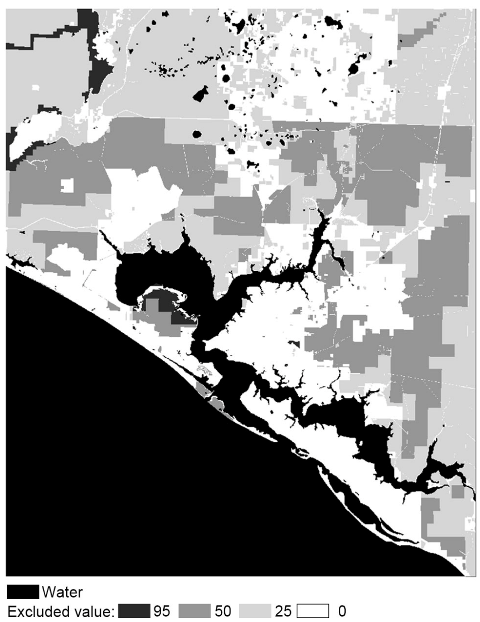

Figure 6. The E2 excluded layer (based on current zoning plans). For the excluded layer, higher value represents higher resistance to urban growth. The value ranges from 0 to 100.

3.2.4 The creation of E3 excluded layer

Most SLEUTH modellers apply the above-mentioned methods to develop excluded layers. However, such methods are deficient since they usually treat the whole study area homogeneously. Conversely, urban growth is more likely to involve heterogeneous changes across the study area. For instance, in coastal regions new residential developments largely extend from existing settlements that may only cover a small portion of the whole study region. Thus, Onsted and Chowdhury (2014) developed a procedure that corrects the growth rates in the AMLEG. The authors concluded that the AMLEG technique produced more accurate results than the other two methods: arbitrary guessing and the calculation based on the whole study area. Therefore, the AMLEG was applied based on the E1 scenario (flooding mitigation). The SLEUTH was run in the prediction mode for 100 Monte Carlo times for the period of 1995 to 2013. All five growth coefficients were set as 100, and the cells with an urbanization probability of 50% or more were considered in the AMELG, as shown in Figure 7.

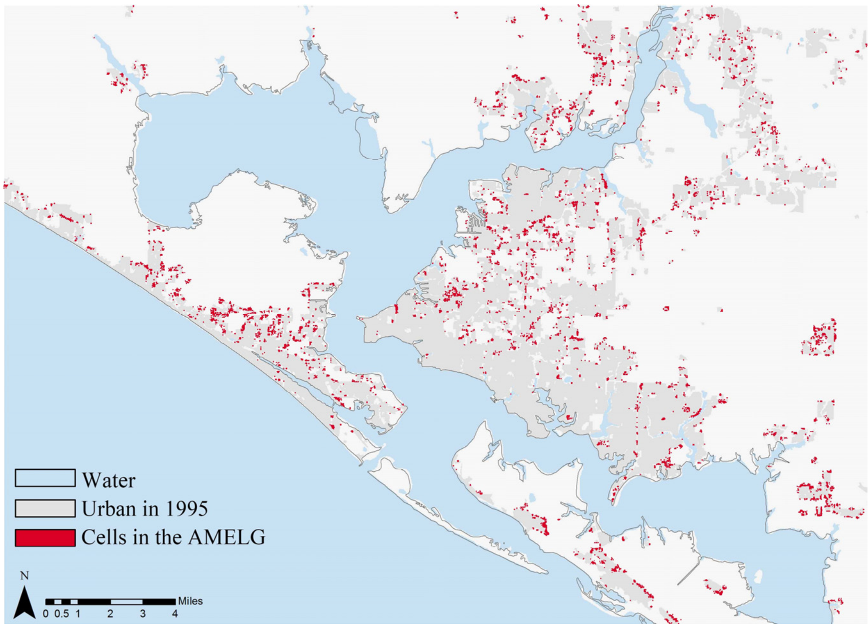

Figure 7. The areas more likely to experience growth (AMLEG) in the coastal region from 1995 to 2013. The cells with 50% or more urbanization probability were considered as AMELG.

Figure 7 shows the coastal areas of high urbanization potentials. The rudimentary simulation of urban growth from 1995 to 2013 justifies the heterogeneous evolution of urban landscape within the whole study region. Thus, the excluded values were re-calculated using the equations (1) and (2), based on the effects of AMLEG (Table 4).

Table 4. The growth rates and excluded values for the E3 layer under the effects of AMLEG.

Zones	New growth from 1995 to 2013 (hectares)	Total area (hectares)	Growth rate (%)	Excluded value
AMLEG	140	513	-	-
SFHA	22	98	1.4	27
Non-SFHA	118	415	1.8	0

The excluded value (27) of the SFHA zone is considerably less than that (68) in the E1 excluded layer. Such a decrease in the excluded value is also found in the study of Onsted and Chowdhury (2014). In addition, this finding indicates that substantial urban growth occurs in flooding-risk areas if the AMLEG effects were considered. This is intuitively reasonable since existing coastal areas are both low-lying places and developmental attractors. Accordingly, the E3 excluded layer was created based on the 2015 FIRM (Figure 8).

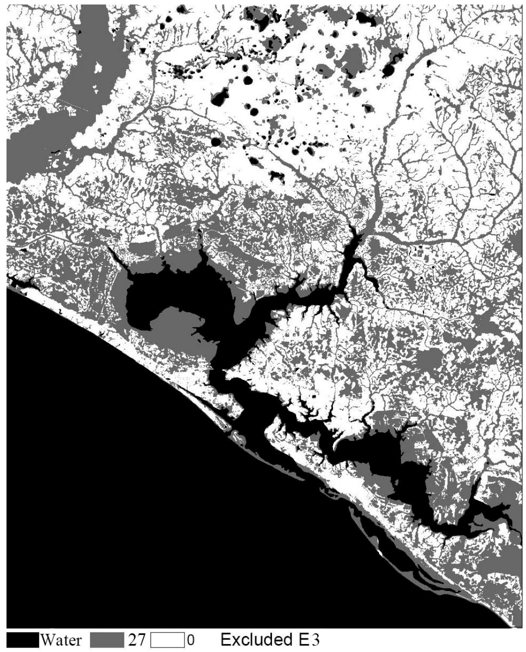

Figure 8. E3 excluded layer (based on the AMLEG technique). The excluded value ranges from 0 to 100. Higher value represents larger resistance to urban growth.

All these raster files were eventually resampled at a spatial resolution of 30 m * 30 m, which is adequately high since the resolutions of most SLEUTH applications are in the range of 10-100m (Akın et al., 2014). These raster files with 1972 rows * 2383 columns were then exported as grayscale GIF images and imported into the SLEUTH program.

3.2.5 Model calibration

As mentioned, urban-growth parameters were calibrated based on the “brute force” technique where four calibration stages---coarse, fine, final, and derive—were followed. Increasingly higher image resolutions were typically used from the coarse to derive calibrations for computational efficiency (Akın et al., 2014; Chakraborty, Wilson, & Kashem, 2015; Rafiee, Mahiny, Khorasani, Darvishsefat, & Danekar, 2009). However, different resolutions may be problematic and lead to a biased estimation of growth patterns (Dietzel & Clarke, 2007; Sekovski et al., 2015). Thus, a consistent resolution of 30 * 30 m was employed during the whole calibration.

In each calibration phase, several Monte Carlo iterations were run to account for the uncertainty associated with parameter estimations. A general strategy of identifying the "best-fit" parameters is to shrink the range of parameters during each stage. Hence, in the coarse calibration four Monte Carlo iterations were conducted, and the widest range of parameters, 0 to 100, were evaluated with an increment of 25 at a time. The goodness-of-fit of models were assessed by thirteen metrics, the majority of which were least-square regression scores between simulated urban components (e.g, increased urban pixels and clusters) and actual counterparts. SLEUTH scholars, however, largely debated the optimal metric which could best describe model performance. Most disputes centred on using single metric or a combination of several indicators. Dietzel and Clarke (2007) developed a composite metric, known as the Optimal SLEUTH Metric (OSM). OSM is the product of the compare, population, edges, clusters, slope, X-mean, and Y-mean metrics and was applied in this work to narrow parameter ranges after each stage.

Seven Monte Carlo iterations with narrower parameter ranges were employed in the fine stage. Further refined parameter ranges with nine Monte Carlo iterations were next tested during the final calibration. This whole process took around one-month CPU time and was conducted using the standard 3.0 SLEUTH model executed in the Cygwin UNIX Windows compiler. This three-stage calibration generated five candidate parameters; however, this set may be biased due to the self-modification nature of SLEUTH. Therefore, a "derive" calibration with the candidate set were performed with 100 Monte Carlo iterations.

3.2.6 Model prediction

Three approaches have been widely applied in model prediction. The first is to adjust growth parameters which affect the way urban growth evolves (i.e., infilling or outward dispersion) (Leao, Bishop, & Evans, 2004; Rafiee et al., 2009; Sekovski et al., 2015). The second is to adjust growth-resistance levels in excluded layers (Jantz, Goetz, Donato, & Claggett, 2010; Sekovski et al., 2015) or apply distinct excluded layers as different policies (Akın et al., 2014). The last one, less frequently used than the first two methods, is to alter self-modification parameters which control overall growth rates (Yang & Lo, 2003). This research used a combination of the first two approaches, and the results were overlaid with SLR induced flooding maps. The urban growth was predicted up to 2080, and the exposure to flooding under different growth patterns and policies were analysed in 2030 and 2080.

As in widespread use in similar studies, this work first simulated three growth patterns: Historical Growth (HUG), Urban Sprawl (USG), and Compact Urban Growth (CUG). HUG assumed that prospective urban extent expanded at existing growth rates. Five parameters remained unchanged over the forecasting period. USG resulted in more scattered urban communities which appeared in suburbs and along transportation corridors. In the model, sprawling growth was controlled by the dispersion, breed, and road gravity, so increasing these parameters produced more dispersed growth. On the contrary, CUG greatly relied on the expansion of current settlements. Compact development is apparent in the study area and many other populated coastal regions. In SLEUTH, compact development was positively associated with spread. In addition, decreasing road gravity inhibited new growth along corridors and thus contributed to compact urban forms.

These growth patterns were next simulated under three policy scenarios: flooding-risk mitigation (E1, based on the whole region), conservational/agricultural land protection (E2), and modified flooding-risk mitigation (E3, based on the AMLEG).

E1 restrained growth in low-lying areas and served as an adaptation strategy to SLR. Alternatively, E2 reflected how future city expansion may be impacted by land use zoning which represented a strong predictor of urban growth in Florida (Jeffrey A. Onsted & Chowdhury, 2014). E3 is a modified scenario of the flooding-risk mitigation based on the fact that urban growth is heterogeneous. Finally, these urban growth predictions were coupled with SLR induced flooding, whose methodology was briefly introduced in the next section.

3.3 Flooding maps

The detailed methodology for generating SLR induced flooding were developed by Hsu (2014). In the hurricane model, the effects of rise in sea level and Sea Surface Temperature (SST) were considered in two stages. First, the increase in SST decreased hurricane central pressure over the sea surface (Knutson & Tuleya, 2004). Changed central pressure and other parameters were next used to calculate projected surge heights using the Surge Response Function (SRF) developed by Irish et al. (2009). Based on this information, a hypothetical hurricane was projected to make landfall at a place where it caused the most damages to coastal areas and resulted in a 500-year flood. Second, the projected surge height for the study region was adjusted by local SLR (Udoh, 2012). Two extreme SLR scenarios were considered, as shown in Table 5. A1F1 corresponded to the highest level of global greenhouse gas emissions (IPCC, 2007). Global data were finally adjusted according to local marine conditions in Panama City.

Table 5. SST Changes and SLR in Two Future Years in Panama City, FL.

Climate Scenario	Rise in SST (℃)	SLR (m)
Present-day	0	0
A1FI (high) in 2030	1.23	0.20
A1FI (high) in 2080	5.02	0.90

The surge heights were calculated in numerous SRF stations which were defined along the coastline of the study area. SRF zones associated with each station were delineated, and each zone had a height value. Eventually, flooding areas were identified by comparing surge heights and local elevation data.

4 Results and discussions

4.1 Model calibration

The multi-stage calibration process generated the following parameters: 71 (dispersion), 92 (breed), 70 (spread), 3 (slope), and 35 (road gravity). High values of the first three parameters suggest that past several decades have witnessed apparent urban sprawl and growth surrounding established settlements. On the contrary, low slope value is intuitively reasonable since the case study region barely has mountainous areas, and therefore slope is not a limiting factor. The impact of major roads is rather limited partly because the road network has remained relatively stable since 1980s.

4.2 Model prediction

Similar studies have suggested that a sensitivity analysis should be conducted before predictions in order to identify the most significant parameter (Sekovski et al., 2015). The assessment was conducted by subsequently setting each parameter as 80 and keeping the others as the lowest value of 1 and running predictions up to 2030. The results indicate that the spread coefficient has the greatest impact upon future urban expansion, resulting in a 13.99% increase in urban areas up to 2030.

Urban sprawl and compact development can be characterized by different sets of parameters. Specifically, urban sprawl is referred to as scatteredly formed settlements and developments along major transportation networks. Conversely, compact developments are in close proximity to existing urban areas. Therefore, two scenarios, urban sprawl (USG) and compact development (CUG), were developed according to the following criteria.

1. The dispersion, breed, and road gravity coefficients were increased and decreased by 25 in USG and CUG respectively.
2. The spread coefficient was risen and lowered by 10 in USG and CUG respectively. Since this parameter was much more influential than the others in terms of urban growth, 10 was selected as an adjusting value in two scenarios.
3. As its impact was quite marginal, slope parameter remained unchanged across all scenarios. Table 6 summarizes different sets of parameters for three scenarios.

Table 6. Growth parameters for three scenarios.

Scenarios	Dispersion	Breed	Spread	Slope	Road gravity
Historical growth	71	92	70	3	35
Urban sprawl	96	100	60	3	60
Compact development	46	67	80	3	10

We applied different parameter combinations into the SLEUTH model and generated various maps which showed the probability of each cell being urbanized. These maps could be then converted to urban / nonurban results by a cut-off probability value. A justified approach to identify the reasonable cut-off value is to assess the histogram frequency of probabilities (Dezhkam, Amiri, Darvishsefat, & Sakieh, 2013; Rafiee et al., 2009; Wu et al., 2008). After evaluating forecasting maps in 2080, we found that there was a steep increase of urbanized cells around the probability of 90%. The cut-off value of 85, accordingly, was selected to determine whether a cell was converted into urban.

The results show that, under no land use regulations, city areas increase substantially under all scenarios (Figure 9 a). For instance, urban region expands up to 826 km^2 in 2080 under the historical growth. Similar patterns can be seen in alternative growth scenarios as well, as shown in Figure 9 a. Under stricter restrictions, the simulations with the E1 excluded layer generate the smallest increase in urban extent from 2013 to 2080 (Figure 9 b). In addition, the growth curves that gradually level off from 2013 indicate a constantly decreasing growth rate. Under compact growth, which shows the most rise in urban areas among three scenarios, the city region expands by 15% within seven decades (Figure 9 b). This is intuitively reasonable because the flooding map exerts a heavy constraint on undeveloped lands, and therefore new developments largely appear near existing settlements. Nonetheless, predictions with the E3 excluded layer produce approximately the same amount of new growth as those with the E1 layer (Figure 9 d). Similarly, urban growth under the conservational/agricultural land protection (E2) has a similar pattern as simulations with no regulations. Figure 9 c shows that the growth rate in compact development reaches the peak (19%) at 2044 and then gradually levels off. Yet, land use zoning does have an impact upon the amount of new urban areas. The simulated urban area in 2080 with the historical growth pattern is 709 km^2 (Figure 9 c), only 85% of that under no restrictions (Figure 9 a). Overall, the results are consistent with similar findings (Sekovski et al., 2015). First, spreading development from existing coastal areas is the leading force behind land use changes. Second, the changes are also driven by dispersion, breed, and road network but less associated with the slope factor.

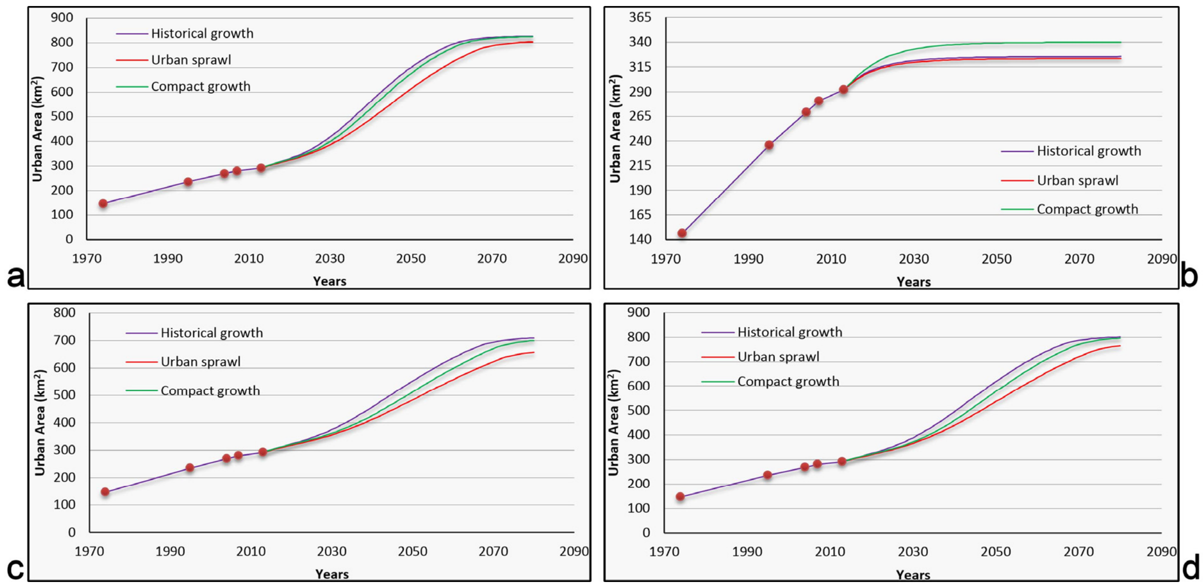

Figure 9. The Simulations of urban changes to the year 2080 of three urban growth patterns under four excluded layers. a) E0: water bodies, b) E1: flooding-risk mitigation (based on the whole region), c) E2: conservational/agricultural land protection, and d) E3: flooding-risk mitigation (based on the AMLEG).

Figure 10 shows predicted urban growth up to 2080 under different excluded layers. These illustrations further depict urban expansion trends indicated by the growth curves in Figure 9. In other words, historical growth and urban sprawl shares similar development patterns where the majority of increased urban cells appear under less strict land use regulations. Moreover, a considerable portion of urban development would be steered towards flooding zones if no land use policy is implemented.

4.3 The exposure of urban growth to flooding risk

Figure 11 shows 500-year flooding maps that would be exacerbated by SLR in 2030 and 2080. A vast region along the West, North, and East Bay would be flooded, and the areas immediate to the West and North Bay would be even more susceptible in 2080. As shown in Table 7, the total inundated area in 2080 would be more than 10 times in 2030. Additionally, affected areas with the flooding depth over 3 m would increase exponentially from 2030 to 2080.

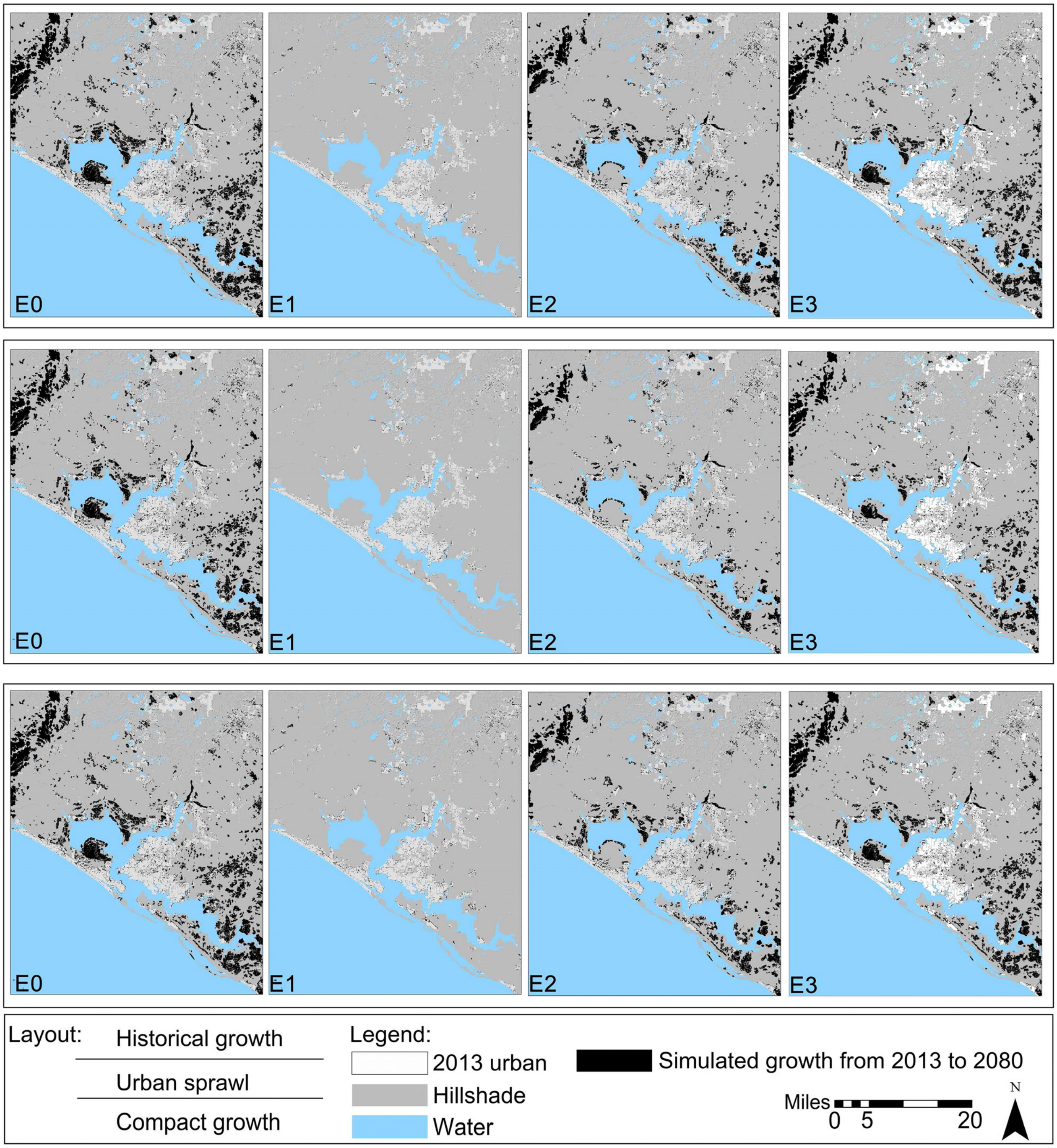

Figure 10. The comparison of modelled urban extent in 2080 with different excluded layers. E0: water bodies, E1: flooding-risk mitigation (based on the whole region), E2: conservational/agricultural land protection, and E3: flooding-risk mitigation (based on the AMLEG).

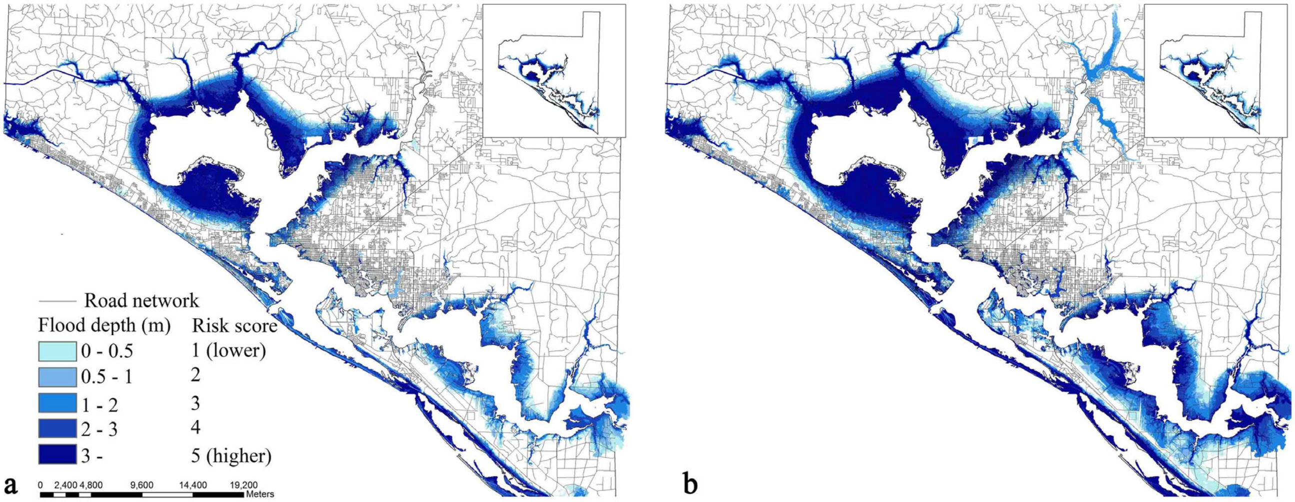

Figure 11. 500-year flood-risk zones of 0.2-m sea level rise (SLR) (a) and 0.9-m SLR (b).

Table 7. Flooded areas under 0.2-m and 0.9-m sea level rise scenarios.

Flooding depth (m)	Area (km^2)	
	0.2-m sea level rise (2030)	0.9-m sea level rise (2080)
0 – 0.5	4.6	58.8
0.5 – 1	4.3	52.5
1 – 2	7.0	100.3
2 – 3	7.0	77.7
Greater than 3	8.2	176.1
Total	31.1	465.4

Future urban growth simulations were overlaid with flooding maps to show how different development patterns guided by distinct policies are vulnerable to SLR induced flooding (Tables 8 – 9). The results show that, if urban growth progresses compactly, total inundated area in 2030 would be the largest among three growth scenarios (Table 8). This finding is echoed by a previous study (Sekovski et al., 2015). In other words, compact development normally appears surrounding existing urban areas, the majority of which are low-lying and prone to flooding. With respect to land use polices, urban growth under regulations leads to less flood-prone development. Specifically, if no regulations are implemented, on average the flooded area in 2080 would be more than 25 times the area under flooding-risk mitigation (Table 9). Both growth patterns and land use policies, accordingly, substantially affect the susceptibility of coastal cities to flooding hazards.

Figure 12 shows how three urban growth scenarios are exposed differentially to SLR induced flooding at a larger geographical scale. First, urban growth is extremely limited if the excluded layer represents the flooding-risk mitigation strategy based on the whole region. Conversely, if water bodies are used as an excluded layer, urban areas expand considerably in coastlines and hinterlands. Noticeably, urban expansion with the E3 excluded layer also generates a vulnerable landscape to flooding. This reflects the heterogeneous developments over the study region. Coastal areas would probably continue to be urbanized even if they are jeopardized by flooding and storm surge. This growth pattern may be partly because the high value of properties along shorelines diminishes SLR impacts. Protective structures along coastlines and flooding insurance programs even attract new developments in flood-prone areas. Second, a vast majority of urbanized areas that would be within flooding polygons are situated in the proximity of the West and North Bay and the shoreline areas of Panama City.

Table 8. The results of overlaying urban growth predictions with the 500-year flooding map in 2030.

Excluded layers	Flooded areas	Urban growth scenarios		
		HUG	USG	CUG
E0: no regulations	Total flooded area (m^2)	59,112,900	57,466,800	59,185,800
	New urban areas that would be flooded (m^2)	7,254,000	5,607,900	7,326,900
E1: flooding-risk mitigation (based on the whole region)	Total flooded area (m^2)	53,223,300	52,974,900	54,468,900
	New urban areas that would be flooded (m^2)	1,364,400	1,116,000	2,610,000
E2: conservational/agricultural land protection	Total flooded area (m^2)	58,479,300	56,867,400	58,603,500
	New urban areas that would be flooded (m^2)	6,620,400	5,008,500	6,744,600
E3: flooding-risk mitigation (based on the AMLEG)	Total flooded area (m^2)	57,974,400	56,486,700	58,048,200
	New urban areas that would be flooded (m^2)	6,115,500	4,627,800	6,189,300

Note: HUG is historical urban growth; USG is urban sprawl growth; and CUG is compact urban growth.

Table 9. The results of overlaying urban growth predictions with the 500-year flooding map in 2080.

Excluded layers	Flooded areas	Urban growth scenarios		
		HUG	USG	CUG
E0: no regulations	Total flooded area (m^2)	200,035,800	185,077,800	199,561,500
	New urban areas that would be flooded (m^2)	116,387,100	101,429,100	115,912,800
E1: flooding-risk mitigation (based on the whole region)	Total flooded area (m^2)	87,068,700	86,526,900	89,570,700
	New urban areas that would be flooded (m^2)	3,420,000	2,878,200	5,922,000
E2: conservational/agricultural land protection	Total flooded area (m^2)	168,683,400	141,254,100	164,392,200
	New urban areas that would be flooded (m^2)	85,034,700	57,605,400	80,743,500
E3: flooding-risk mitigation (based on the AMLEG)	Total flooded area (m^2)	181,416,600	155,827,800	179,401,500
	New urban areas that would be flooded (m^2)	97,767,900	72,179,100	95,752,800

Note: HUG is historical urban growth; USG is urban sprawl growth; and CUG is compact urban growth.

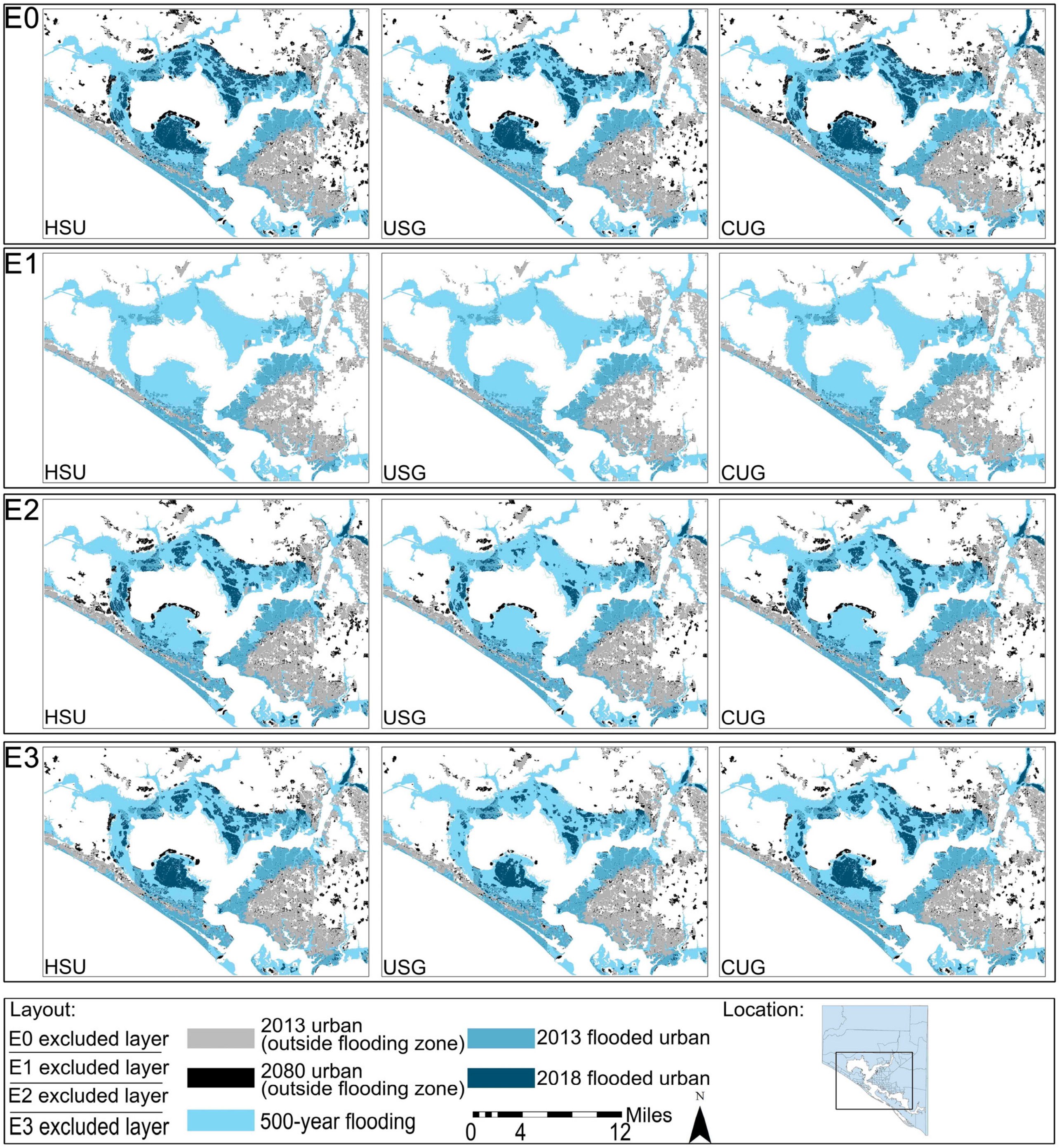

Figure 12. Flooded urban extent in 2080. E0: water bodies, E1: flooding-risk mitigation (based on the whole region), E2: conservational/agricultural land protection, E3: flooding-risk mitigation (based on the AMLEG), HSU: historical growth, USG: urban sprawl, and CUG: compact development

4.4 Discussion

4.4.1 Urban growth and coastal hazards

The calibration results indicate that main driving force for the study area is spread, followed by dispersion and breed. Such findings are consistent with similar coastal studies (Sakieh et al., 2015; Sekovski et al., 2015). In other words, urban growth is likely to take place around current settlements in a compact fashion. Existing settlements are featured by high accessibility to infrastructure, activity centers, and coastal amenities. Additionally, a multitude of new urban areas cluster around coastlines, which is evident either under historical growth or urban sprawl scenarios. Increased human activities and the competition for limited resources, therefore, intensify environmental pressures at land-sea interfaces. Furthermore, the interface faces unprecedented threats from SLR and other intensified coastal hazards. SLEUTH could provide useful information about future urban growth and thus benefit coastal city managers and land use planners.

However, urban growth models have their own limitations. The most noticeable one is their inability of capturing the whole range of factors affecting urbanization (Herold, Goldstein, & Clarke, 2003). The demand for urban growth comes from population and economic increase. The Bureau of Economic and Business Research at the University of Florida (2016) forecasts that the total population of Bay County will increase by almost 40% by 2030. Such an apparent rise probably demands significant urbanization. Therefore, socioeconomic factors behind urbanization should be considered in applications. Population increase, however, is linked with migration, overall economic conditions, and other factors, which is complicated and hard to predict. Additionally, urbanization in coastal regions is driven by economic activities, the majority of which are related to tourism and real estate. Nevertheless, barely are these factors taken into account in CA models. Third, urban growth predictions may be biased if modellers fail to justify the values in excluded layers. This study determined the excluded values of E2 scenario according to future land use plans and suggestions from other studies (e.g., Akin et al., 2014). Although the lack of historical zoning information forced us to make this assumption, the predictions under the E2 scenario may become problematic.

When urban growth models are coupled with coastal hazards that are associated with SLR, additional concerns arise. In SLEUTH, urban growth predictions fail to incorporate seawall, population relocation, and other adaptation strategies to SLR. This limitation can be seen in the given examples of future flooding risks (Figure 12). Considerable existing urban areas would fall into flooding polygons in 2030 and 2080. Essentially, the model assumes a “do-nothing” option regarding adaptation strategies, which may be improved in future research. Another uncertainty arises during the development of SLR induced flooding. In other words, researchers have not yet reached an agreement as to SLR predictions. Sea level may possibly increase more rapidly than people initially thought. Nicholls and Cazenave (2010) reviewed numerous prediction sources and concluded that global mean sea level would rise between 0.19 m and 1.7 m by 2100. Given these uncertainties, therefore, the simulation results should be interpreted with extreme carefulness and objectivity. In addition, the extrapolation of future urban growth beyond the calibration range can be questionable and generate uncertain results (Goldstein, Candau, & Clarke, 2004). Modellers ought to make a trade-off between urban predictions and the forecasts of climate change related hazards. Climate change is slow going, but urbanization may be rapid in populated coastal regions. For instance, SLR may become significant only after an adequate time frame that probably exceeds the time period of historical urban data. Such coupled analyses should aim at identifying the general impacts of climate change on prospective urbanization, rather than replicating past patterns of urban development.

4.4.2 Policy implications

Compact urban forms are advocated because of their environmental friendliness and energy conservation (Dezhkam et al., 2013; A. Mahiny & Gholamalifard, 2007). Yet, this might not be true in flat coastal areas from the perspective of hazard mitigation. As indicated in Tables 8 and 9, the compact growth model generates more extension of current flood-prone areas than historical growth and urban sprawl. For instance, if the flooding-risk mitigation is implemented, new urban areas that would be flooded in 2030 under the compact growth pattern are over 2,500,000 m^2, almost double the area under historical growth scenario. However, such conclusions are made only based on our case study area where the elevation is low and change insignificantly. The effects of compact urban forms on regional exposure to flooding require further investigation in other coastal regions with different topographical features. Therefore, it is recommended that spontaneous urban growth should be regulated to prevent farmland loss, and urban development should be also oriented towards hinterland that already has appreciable urban areas.

Population and economic growth largely drive urban growth. Yet, policies behind such growth should also be investigated since land use plans and economic strategies represent developmental blueprints. Thus, it is beneficial to reflect upon different policies contributing to distinct urban growth patterns: urban sprawl and compact growth. Urban sprawl is characterised by unplanned and scattered developments in suburban areas. Uncoordinated growth in the city edge has been suggested to be associated with multidimensional factors regarding economic incentives, housing development plans, and transportation policies (De Vos & Witlox, 2013; Lopez & Hynes, 2003; Yue, Zhang, & Liu, 2016). Economic incentive packages launched by the central government have contributed to urban sprawl in the developing world. For instance, China took economic reform in 1970s by opening up land markets and commercializing housing units. This economic stimulus gave rise to many sprawling mega-cities such as Beijing, Shanghai, and Chengdu. In Europe and North America, micro-economic theories may explain urban sprawl. Households begin to relocate to the suburbs when the land prices in city centers become prohibitively high. Their relocation decisions are further strengthened by housing and land development policies. Developers promote low-density communities in the city periphery. Local governments help to build large retail centers to accommodate the increased demand. Motorization policies and low fuel costs result in automobile-oriented cities. Even public transit policies aggravate outward city growth by charging long-distance commuters less than riders for short distances (De Vos & Witlox, 2013). As urban sprawl increasingly threatens public health, social equity, and the built environments, people start to develop different urban containment policies. There are primarily two forms of containment policies that were adopted in the US. The State law in Oregon and Washington requires that local land-use plans should clearly define an urban growth boundary. In other states such as Florida and Maryland, governments develop urban service limits, public facilities ordinances, and other policies to promote compact urban forms (Aytur, Rodriguez, Evenson, & Catellier, 2008). However, the effects of urban containment policies have been hotly debated. For example, not all urban growth boundaries significantly affect housing markets and urbanization paces (Dempsey & Plantinga, 2013). Thus, De Vos and Witlox (2013) suggest the integration of spatial planning policies, mobility policies, and road pricing. Spatial planning can strictly limit new developments outside urban areas. The development of Transit-Oriented Development benefits nurturing high-density and mixed land-use neighbourhoods. In addition, road pricing increases long-distance travel costs, thereby curtailing urban sprawl.

The modelling approach and results offered by this work could aid in the development of an integral land-use enforcement system. Building an integrated land use policy for the urban growth landscape is a recommended option in coastal communities. An integrative policy framework can coordinate the increased demand for urbanization and the goal for hazard mitigation. In addition, land use zoning for existing coastal areas should be incorporated with adaptation strategies to SLR. Rural land use management and regulations should be oriented in order to attract new development inland. While the prohibition of development within flooding zones greatly constrains urban growth and is therefore unrealistic, only relying on land use zoning could lead to considerable inundated urban areas. A compromise of these two alternatives, accordingly, could be developed to ensure adequate urbanization and steer new developments away from low-lying areas. Finally, seawall, planned retreat, and other adaptation strategies should be incorporated in the framework to protect existing urban areas from flooding risks. In the long term, adaptation plans ought to consider other SLR aspects such as groundwater pollution and saltwater intrusion beneath protective structures.

5 Conclusions

Environmental and resource pressures are increasingly intensified given ongoing coastal urbanization. In addition, urbanization process amplifies the exposure of coastal communities to flooding hazards. Furthermore, we are uncertain about the degree to which SLR may contribute to the increased intensity of storminess. The possibility of more exacerbated consequences, however, cannot be neglected from a precautionary perspective. Therefore, it is crucial to building an effective coastal management plan to balance land use, competing interests, and hazard mitigation.

This work contributes to the literature by integrating urban growth dynamics, land use policies, and SLR induced flooding. We successfully calibrated the SLEUTH model for Bay County coastal areas, Florida, based on historical data from the year 1974 to 2013. By applying the best-fit coefficients we developed three urban growth scenarios and assessed the exposure of future urban extent to SLR induced flooding under different land use policies. These scenarios reflected various growth strategies widely applied in urban planning. Our results indicate that urban growth is mainly driven by the parameter of compact development. The results show that substantial urban growth would be prone to coastal flooding if no land use policy is implemented.

SLEUTH is particularly useful in modelling complex spatial dynamics. In addition, the computational capacity of SLEUTH is greatly enhanced due to rapid advancement of computer technologies. By outputting GIF maps and statistics for each prediction year, SLEUTH can be easily linked with a raster-based GIS environment (Rafiee et al., 2009). Therefore, the results of different scenarios can be readily imported into a GIS platform for presentation purposes. The coupled model serves as a decision support tool and helps city managers, land use planners, and hazard mitigation teams evaluate the outcomes of different policies. Additionally, the visualization results can be used to raise general awareness about the vulnerability of coastal communities to SLR.

Admittedly, the model is just a simplification of reality, and urban growth is an intricate process that involves population increase, economic activities, and many other factors. Since the level of SLR impact on flooding is quite unclear, and growth predictions could be probably biased, the model cannot generate exact results of urban growth and flooding extent. However, we believe that "what-if" estimations are useful in helping decision makers understand how different developments may be oriented. Therefore, probabilistic models and scenario-based planning should be advocated in order to evaluate planning alternatives and their consequences (Xiang & Clarke, 2003) as well as offer reliable estimates of flooding damages.

Acknowledgements

The authors thank Dr. Keith C. Clarke for his help on the model calibration process. The authors also thank the U.S. Census Bureau, the Florida Geographic Data Library, the Bay County Online, and the Bureau of Economic and Business Research for offering access to data. This paper was undertaken with support from the Florida Sea Grant, Grant No. R/GOM-RP-2, "A Parameterized Climate Change Projection Model for Hurricane Flooding, Wave Action, Economic Damages, and Population Dynamics". This paper was also funded by the Florida Sea Grant Project entitled "A Spatial-Temporal Econometric Model to Estimate Costs and Benefits of Sea-Level Rise Adaptation Strategies".

References

Akın, A., Clarke, K. C., & Berberoglu, S. (2014). The impact of historical exclusion on the calibration of the SLEUTH urban growth model. *International Journal Of Applied Earth Observation And Geoinformation, 27, Part B*(0), 156-168. doi:http://dx.doi.org/10.1016/j.jag.2013.10.002

Aytur, S. A., Rodriguez, D. A., Evenson, K. R., & Catellier, D. J. (2008). Urban Containment Policies and Physical Activity: A Time–Series Analysis of Metropolitan Areas, 1990–2002. *American Journal of Preventive Medicine, 34*(4), 320-332. doi:http://dx.doi.org/10.1016/j.amepre.2008.01.018

Bay County Online. (2016). Future land use and zoning. Retrieved from http://www.baycountyfl.gov/gis.php

Bureau of Economic and Business Research. (2015). Spending on Tourism in Florida. Retrieved from https://www.bebr.ufl.edu/ecodb/localities/3739/msa

Bureau of Economic and Business Research. (2016). Total population in Bay County. Retrieved from https://www.bebr.ufl.edu/population

Chakraborty, A., Wilson, B., & Kashem, S. b. (2015). The pitfalls of regional delineations in land use modeling: Implications for Mumbai region and its planners. *Cities, 45*, 91-103. doi:http://dx.doi.org/10.1016/j.cities.2015.03.008

Clarke, K. C., Hoppen, S., & Gaydos, L. (1997). A Self-Modifying Cellular Automaton Model of Historical Urbanization in the San Francisco Bay Area. *Environment and Planning B: Planning and Design, 24*(2), 247-261. doi:10.1068/b240247

De Vos, J., & Witlox, F. (2013). Transportation policy as spatial planning tool; reducing urban sprawl by increasing travel costs and clustering infrastructure and public transportation. *Journal Of Transport Geography, 33*, 117-125. doi:http://dx.doi.org/10.1016/j.jtrangeo.2013.09.014

Dempsey, J. A., & Plantinga, A. J. (2013). How well do urban growth boundaries contain development? Results for Oregon using a difference-in-difference estimator. *Regional Science and Urban Economics, 43*(6), 996-1007. doi:http://dx.doi.org/10.1016/j.regsciurbeco.2013.10.002

Dezhkam, S., Amiri, B. J., Darvishsefat, A. A., & Sakieh, Y. (2013). Simulating the urban growth dimensions and scenario prediction through sleuth model: a case study of Rasht County, Guilan, Iran. *GeoJournal, 79*(5), 591-604. doi:10.1007/s10708-013-9515-9

Dietzel, C., & Clarke, K. C. (2007). Toward optimal calibration of the SLEUTH land use change model. *Transactions in GIS, 11*(1), 29-45. doi:10.1111/j.1467-9671.2007.01031.x

Felsenstein, D., & Lichter, M. (2014). Introduction to the special issue on simulating the dynamics of land use change in coastal areas. *Ocean & Coastal Management, 101, Part B*, 61-62. doi:http://dx.doi.org/10.1016/j.ocecoaman.2014.09.014

Florida Geographic Data Library. (2016). Retrieved from http://www.fgdl.org/metadataexplorer/explorer.jsp

Garcia, E. S., & Loáiciga, H. A. (2014). Sea-level rise and flooding in coastal riverine flood plains. *Hydrological Sciences Journal, 59*(1), 204-220. doi:10.1080/02626667.2013.798660

Goldstein, N. C., Candau, J. T., & Clarke, K. C. (2004). Approaches to simulating the "March of Bricks and Mortar". *Computers, Environment and Urban Systems, 28*(1–2), 125-147. doi:http://dx.doi.org/10.1016/S0198-9715(02)00046-7

Hansen, H. S. (2010). Modelling the future coastal zone urban development as implied by the IPCC SRES and assessing the impact from sea level rise. *Landscape and Urban Planning, 98*(3–4), 141-149. doi:http://dx.doi.org/10.1016/j.landurbplan.2010.08.018

Herold, M., Goldstein, N. C., & Clarke, K. C. (2003). The spatiotemporal form of urban growth: measurement, analysis and modeling. *Remote Sensing of Environment, 86*(3), 286-302. doi:http://dx.doi.org/10.1016/S0034-4257(03)00075-0

Hsu, C.-H. (2014). *Hurricane Surge Flooding Damage Assessment and Web-Based Game Development to Support K12 Education for Understanding Climate Change Impact on Hurricane Surge Flooding Damage.* (Doctoral dissertation), Texas A & M University. Retrieved from http://hdl.handle.net/1969.1/153484

Hurricanecity. (2015). The history with tropical systems in Panama City, Florida. Retrieved from http://www.hurricanecity.com/city/panamacity.htm

IPCC. (2007). Climate change 2007: the physical science basis. *Summary for Policymakers*.

IPCC. (2013). *Summary for Policymakers. In: Climate Change 2013: The Physical Science Basis. Contribution of Working Group I to the Fifth Assessment Report of the Intergovernmental Panel on Climate Change [Stocker, T.F., D. Qin, G.-K. Plattner, M. Tignor, S.K. Allen, J. Boschung, A. Nauels, Y. Xia, V. Bex and P.M. Midgley (eds.)]*. Cambridge, United Kingdom and New York, NY, USA: Cambridge University Press.

Irish, J. L., Resio, D. T., & Cialone, M. A. (2009). A surge response function approach to coastal hazard assessment. Part 2: Quantification of spatial attributes of response functions. *Natural Hazards, 51*(1), 183-205.

Jantz, C. A., Goetz, S. J., Donato, D., & Claggett, P. (2010). Designing and implementing a regional urban modeling system using the SLEUTH cellular urban model. *Computers, Environment and Urban Systems, 34*(1), 1-16. doi:http://dx.doi.org/10.1016/j.compenvurbsys.2009.08.003

Knutson, T. R., & Tuleya, R. E. (2004). Impact of CO2-induced warming on simulated hurricane intensity and precipitation: Sensitivity to the choice of climate model and convective parameterization. *Journal of Climate, 17*(18), 3477-3495.

Leao, S., Bishop, I., & Evans, D. (2004). Simulating Urban Growth in a Developing Nation's Region Using a Cellular Automata-Based Model. *Journal of Urban Planning and Development, 130*(3), 145-158. doi:10.1061/(ASCE)0733-9488(2004)130:3(145)

Leão, S., Bishop, I., & Evans, D. (2004). Spatial–temporal model for demand and allocation of waste landfills in growing urban regions. *Computers, Environment and Urban Systems, 28*(4), 353-385. doi:http://dx.doi.org/10.1016/S0198-9715(03)00043-7

Lopez, R., & Hynes, H. P. (2003). Sprawl In The 1990s: Measurement, Distribution, and Trends. *Urban Affairs Review, 38*(3), 325-355. doi:10.1177/1078087402238805

Mahiny, A., & Gholamalifard, M. (2007). Dynamic spatial modeling of urban growth through cellular automata in a GIS environment.

Mahiny, A. S., & Clarke, K. C. (2012). Guiding SLEUTH Land-Use/Land-Cover Change Modeling Using Multicriteria Evaluation: Towards Dynamic Sustainable Land-Use Planning. *Environment and Planning B: Planning and Design, 39*(5), 925-944. doi:10.1068/b37092

Nicholls, R. J., & Cazenave, A. (2010). Sea-level rise and its impact on coastal zones. *Science, 328*(5985), 1517-1520.

Onsted, J., & Clarke, K. C. (2012). The inclusion of differentially assessed lands in urban growth model calibration: a comparison of two approaches using SLEUTH. *International Journal of Geographical Information Science, 26*(5), 881-898. doi:10.1080/13658816.2011.617305

Onsted, J. A., & Chowdhury, R. R. (2014). Does zoning matter? A comparative analysis of landscape change in Redland, Florida using cellular automata. *Landscape and Urban Planning, 121*(0), 1-18. doi:http://dx.doi.org/10.1016/j.landurbplan.2013.09.007

Onsted, J. A., & Clarke, K. C. (2011). Forecasting Enrollment in Differential Assessment Programs Using Cellular Automata. *Environment and Planning B: Planning and Design, 38*(5), 829-849. doi:10.1068/b37010

Project Gigalopolis. (2016). SLEUTH Applications Retrieved from http://www.ncgia.ucsb.edu/projects/gig/Repository/SLEUTHapplications.html

Rafiee, R., Mahiny, A. S., Khorasani, N., Darvishsefat, A. A., & Danekar, A. (2009). Simulating urban growth in Mashad City, Iran through the SLEUTH model (UGM). *Cities, 26*(1), 19-26. doi:http://dx.doi.org/10.1016/j.cities.2008.11.005

Rienow, A., & Goetzke, R. (2015). Supporting SLEUTH – Enhancing a cellular automaton with support vector machines for urban growth modeling. *Computers, Environment and Urban Systems, 49*(0), 66-81. doi:http://dx.doi.org/10.1016/j.compenvurbsys.2014.05.001

Runyan, R. C. (2006). Small business in the face of crisis: Identifying barriers to recovery from a natural disaster. *Journal of Contingencies and Crisis Management, 14*(1), 12-26.

Sakieh, Y., Salmanmahiny, A., Jafarnezhad, J., Mehri, A., Kamyab, H., & Galdavi, S. (2015). Evaluating the strategy of decentralized urban land-use planning in a developing region. *Land Use Policy, 48*, 534-551. doi:http://dx.doi.org/10.1016/j.landusepol.2015.07.004

Santé, I., García, A. M., Miranda, D., & Crecente, R. (2010). Cellular automata models for the simulation of real-world urban processes: A review and analysis. *Landscape and Urban Planning, 96*(2), 108-122. doi:http://dx.doi.org/10.1016/j.landurbplan.2010.03.001

Sekovski, I., Armaroli, C., Calabrese, L., Mancini, F., Stecchi, F., & Perini, L. (2015). Coupling scenarios of urban growth and flood hazards along the Emilia-Romagna coast (Italy). *Natural Hazards and Earth System Sciences, 15*(10), 2331-2346. doi:10.5194/nhess-15-2331-2015

Shows, E. W. (1978). Florida's coastal setback line—an effort to regulate beachfront development. *Coastal Management, 4*(1-2), 151-164.

Song, J., Peng, Z.-R., Zhao, L., & Hsu, C.-H. (2016). Developing a theoretical framework for integrated vulnerability of businesses to sea level rise. *Natural Hazards*, 1-21. doi:10.1007/s11069-016-2483-x

U.S. Census Bureau. (2015). Total Population in Bay County. Retrieved from http://factfinder.census.gov/faces/tableservices/jsf/pages/productview.xhtml?pid=DEC_10_SF1_P1&prodType=table

U.S. Census Bureau. (2016). TIGER/Line shapefiles and TIGER/Line Files. Retrieved from http://www.census.gov/geo/maps-data/data/tiger-line.html

Udoh, I. E. (2012). *Robust hurricane surge response functions*: TEXAS A&M UNIVERSITY.

Wagner, D. F. (1997). Cellular Automata and Geographic Information Systems. *Environment and Planning B: Planning and Design, 24*(2), 219-234. doi:10.1068/b240219

White, R., & Engelen, G. (2000). High-resolution integrated modelling of the spatial dynamics of urban and regional systems. *Computers, Environment and Urban Systems, 24*(5), 383-400. doi:http://dx.doi.org/10.1016/S0198-9715(00)00012-0

Wu, X., Hu, Y., He, H. S., Bu, R., Onsted, J., & Xi, F. (2008). Performance Evaluation of the SLEUTH Model in the Shenyang Metropolitan Area of Northeastern China. *Environmental Modeling & Assessment, 14*(2), 221-230. doi:10.1007/s10666-008-9154-6

Xiang, W.-N., & Clarke, K. C. (2003). The Use of Scenarios in Land-Use Planning. *Environment and Planning B: Planning and Design, 30*(6), 885-909. doi:10.1068/b2945

Yang, X., & Lo, C. P. (2003). Modelling urban growth and landscape changes in the Atlanta metropolitan area. *International Journal of Geographical Information Science, 17*(5), 463-488. doi:10.1080/1365881031000086965

Yue, W., Zhang, L., & Liu, Y. (2016). Measuring sprawl in large Chinese cities along the Yangtze River via combined single and multidimensional metrics. *Habitat International, 57*, 43-52. doi:http://dx.doi.org/10.1016/j.habitatint.2016.06.009